

2. Rotating Fields in Electric Machines

Machines with rotating fields are an important part of rotating converters of electric into mechanical energy and vice versa. This electromechanical energy conversion takes place via rotating magnetic fields. The most important machines with rotating fields are **synchronous and asynchronous machines**, that are widely distributed in the areas of electrical energy generation and modern drives systems.

In principle, every rotating magnetic field is a rotating field, e.g., also the magnetic field of a rotating permanent magnet horseshoe magnet and the bundled magnetic beam of a pulsar (rapidly rotating neutron star). Here, the rotating magnetic field in the air gap between the stator and the rotor of an electric machine is meant. It is generated by a system of **current-carrying, stationary** coils that are placed in the slots of the stator core lamination. The present chapter deals with the realisation and the mathematical analysis of such a rotating field.

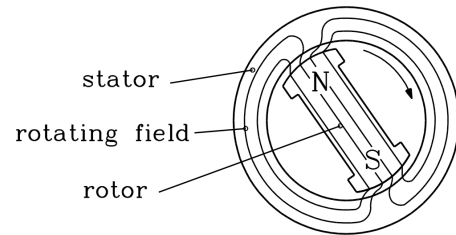


Fig. 2.1: A rotating magnetic field pulls a freely pivotable bar magnet (rotor).

2.1 Basic Principles of Calculation of Magnetic Fields

a) Basic Principles:

The calculation of electromagnetic fields is done by means of the **four equations of MAXWELL** (2.1) – (2.4), using the corresponding **constitutive relations** (2.5) – (2.7) (overview of symbols in Chapter 1!).

$$\text{curl} \vec{H} = \vec{J} + \frac{\partial \vec{D}}{\partial t} \quad (2.1)$$

$$\text{curl} \vec{E} = -\frac{\partial \vec{B}}{\partial t} \quad (2.2)$$

$$\text{div} \vec{B} = 0 \quad (2.3)$$

$$\text{div} \vec{D} = \rho \quad (2.4)$$

$$\vec{J} = \kappa \cdot \vec{E} \quad (2.5)$$

$$\vec{B} = \mu \cdot \vec{H} = \mu_0 \vec{H} + \mu_0 \vec{M} = \mu_0 \vec{H} + \vec{J}_M \quad (2.6)$$

$$\vec{D} = \epsilon \cdot \vec{E} \quad (2.7)$$

In the context of electric machines, **mainly fields varying slowly with time** have to be considered (rate of change typically 50 Hz up to several kHz). Therefore, the rate of change of the dielectric flux density \vec{D} with time in (2.1) can be neglected (2.8).

$$\text{curl} \vec{H} = \vec{J} \quad (2.8)$$

Electric source fields \vec{D} or \vec{E} according to (2.4) concern mainly the voltage stress of the winding insulation, whereas electric eddy fields \vec{E} according to (2.2) describe the voltage induction in electric machines.

Results:

Equations (2.8) and (2.3) allow the calculation of the magnetic fields B and H . They are to be combined using the constitutive relation (2.6) for the iron parts of stator and rotor.

In the following, the electric current density in the coils of the electric conductors \vec{J} is considered as externally impressed and the **magnetic field density** \vec{H} calculated based on it. In the air gap, \vec{H} is identical with the **magnetic induction** \vec{B} (flux density), except for the factor $\mu_0 = 4\pi \cdot 10^{-7} \text{ Vs/(Am)}$ (**permeability of vacuum**). In the iron parts, the magnetisation \vec{M} , respectively the magnetic polarisation \vec{J}_M of the material increase the magnetic field \vec{H} , resulting in a much higher value of \vec{B} than in air. Physically, this is done by the alignment of the microscopically small elementary areas of the iron (**WEISS' domain**) that contain some magnetic remanence when submitted to an external field \vec{H} . In electric machines this field is generated by the current flow in the coils. If all elementary areas are aligned in parallel to the external field \vec{H} , the iron is "**saturated**". A further increase of the field only results in an increase of the external field as if it was in air. With iron, this is the case above a flux density \vec{B} of about 1.7 – 1.8 T. Therefore, the rated flux density in the iron of electric machines is not much larger than 2.0 – 2.2 T. The constitutive relation (2.6) is **non linear** (2.9).

$$\vec{B} = \mu(H) \cdot \vec{H} \quad (2.9)$$

The parameter "permeability of iron" μ depends of \vec{H} . At small values of \vec{B} , respectively of \vec{H} , it is typically 5000 times as large as μ_0 . However, at values higher than 2.5 T, it approaches the value of μ_0 due to the above mentioned saturation.

b) Integral Basic Principles:

Here, equations (2.8) and (2.3) are not used in the form of differential, but in the form of integral equations. The transfer from one into the other form is done using the **laws of integrals**.

b1) AMPERE's Circuital Law:

According to **STOKES's** law of integrals, equation (2.10) is true for any field of vectors \vec{H} that pass through an area A enclosed by a loop C (Fig. 2.1) :

$$\int_A \text{curl} \vec{H} \cdot d\vec{A} = \oint_C \vec{H} \cdot d\vec{s} \quad (2.10)$$

This means: The integral along a curve of the magnetic field \vec{H} along the closed loop C spanning the area A equals the surface integral of the $\text{curl} \vec{H}$ along the area A . According to (2.8), the curl of \vec{H} equals the current density \vec{J} of the electric conductor. The integral of the area of \vec{J}

$$\int_A \vec{J} \cdot d\vec{A} = \Theta$$

equals the sum of all currents (“**current linkage**” Θ , also considered as “ampère-turns”), that passes through the area A . This results in *MAXWELL*’s first law in integral form, the so-called *AMPÈRE*’s circuital law:

$$\oint_C \vec{H} \cdot d\vec{s} = \Theta \quad (2.11)$$

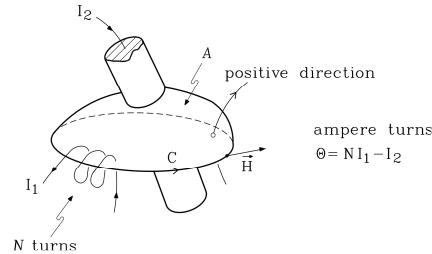


Fig. 2.2: Closed loop C around current-carrying conductor, currents I_1, I_2 . The loop C can be chosen arbitrarily, hence, it does not have to be along a field line of \vec{H} .

Example 2.1-1:

Area and winding arrangement according to Fig. 2.2: The current linkage is $\Theta = N \cdot I_1 - I_2$, because the number of windings values N for the first and 1 for the second circuit, and the two currents flow in opposite directions. The current I_1 passes the area according to the right-hand-rule with a positive orientation.

b2) GAUSS’s Law on the magnetic flux through a closed surface:

According to *GAUSS*’s law of integrals (Fig 2.3), the integral of an area of any field of vectors \vec{B} along a closed surface A of a volume V equals the total charge (total strength of the source, divergence) $\text{div}\vec{B}$ of the flux density in the considered volume V .

$$\int_V \text{div}\vec{B} \cdot dV = \oint_A \vec{B} \cdot d\vec{A} \quad (2.12)$$

Using (2.3), the third law of *MAXWELL* for the magnetic flux density B is given in integral form, which is known as the **law of the magnetic flux through a closed surface**: The flux through a closed surface is always zero!

$$\oint_A \vec{B} \cdot d\vec{A} = \Phi = 0 \quad (2.13)$$

This means, that as much **magnetic flux** Φ enters the volume V as it leaves V , because the total flux of the closed surface A values zero. Accordingly, the tubes of \vec{B} (in two dimensions: the “flux lines” of \vec{B}) are closed loops (Fig. 2.3). Therefore, the component B_n that is normal to the area A is the same inside and outside of the volume (**constancy of the normal component of B**):

$$B_{n,1} = B_{n,2} \quad (2.13a)$$

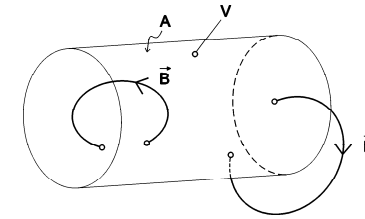


Fig. 2.3: As many flux tubes of \vec{B} leave the volume V as enter V .

Regions with leaving flux tubes are considered as “north poles”, regions with entering flux tubes as “south poles”. Therefore, (2.13) signifies that **north and south poles only exist together**. A magnetic mono-pole has not been discovered until today. Any magnetic field – also the one of electric machines – is at least a dipole field. The minimum number of poles is 2 (one north and one south pole). The number of magnetic poles is $2p$ (**number of pole pairs** $p = 1, 2, 3, \dots$).

2.2 Simplified Calculation of the Air gap Field of Electric Machines

a) Simplifying Assumptions:

Modern numerical methods of calculation, e.g. the “finite differences”, “finite elements” and the “boundary elements” methods solve *MAXWELL*’s differential equations and the non-linear constitutive relations and allow a detailed calculation of the magnetic fields in electric machines. However, **simplified analytical calculations** are sufficient for the understanding and rough calculations of the fields. These are presented in the following. A number of simplifying assumptions is essential for these analytical calculations:

- The iron is considered to be only slightly saturated or not saturated at all. Then, **μ can be assumed to be infinite**. In this case, the flux lines of B enter the iron almost perpendicularly because of $\mu \gg \mu_0$.
- The width of the **air gap** δ of electric machines is much smaller than the width of one pole (pole pitch). Therefore, the field in the air gap contains only a radial component.
- The axial length of the machine l_{Fe} is much larger than δ . Therefore, **effects at the boundaries**, e.g. flux tubes that leave the cylindrical rotor via the face surface and enter the stator lamination via the face surface of the stator (end winding leakage), can be neglected when compared with the air gap flux.
- The slots that contain the coils are considered infinitely small (**concentrated current flow in the slots**).

b) Air Gap Field of a Current-Conduction Coil:

The **axial cross-sectional area of a two pole electric machine** with an electric winding in the stator with a single coil (number of turns per coil N_c , coil current I_c) that is excited with the ampere-turns Θ (Fig 2.4) is considered. As it is $B_{n,1} = B_{n,2}$, \vec{B} in the air gap is as large as in the directly adjacent iron part. As the permeability of iron μ_{Fe} is infinitely large, $\vec{H}_{Fe} = \vec{B} / \mu_{Fe}$ has to be zero in the iron. Therefore, the parts of the loop integral of (2.11) of the stator and rotor iron are zero and only the two parts of the air gap are left for calculation. \vec{H} remains almost constant along the air gap width δ , as δ is very small. H is denoted as H_δ , which is the radial component of the vector field \vec{H} in the air gap.

Therefore, it is (with A_{Fe} as the iron path of a flux line along a loop C):

$$\oint_C \vec{H} \cdot d\vec{s} = 2H_{Fe}A_{Fe} + 2H_{\delta}\delta = 2H_{\delta}\delta = \Theta \quad (2.14)$$

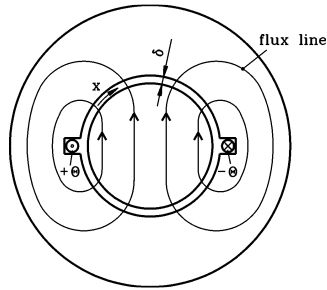


Fig. 2.4: Coil carrying the ampere turns Θ that excites the two pole magnetic field \vec{B} (shown: cross sectional area of an electric machine)

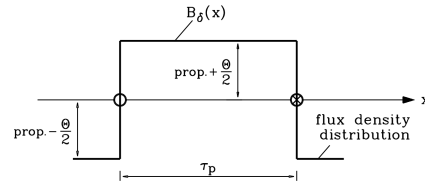


Fig. 2.5: Distribution of magnetic flux density in the air gap along the circumference of the machine

As the air gap width δ is almost constant along the circumference of the machine (the influence of the slot openings is neglected), H_{δ} and therefore $B_{\delta} = \mu_0 H_{\delta}$ are constant and have positive sign along half of the circumference (upper half of the machine) and constant with negative sign along the other half of the circumference (lower half of the machine). Therefore, the circumference of the machine in the air gap $d_{si}\pi$ (d_{si} : stator inner diameter = “**bore diameter**”) is divided in two identical parts, the **pole pitches** τ_p , where B_{δ} has either positive (north pole) or negative (south pole) sign. For any number of pole pairs $2p$, it is:

$$\tau_p = \frac{d_{si}\pi}{2p} \quad (2.15)$$

In the air gap, the **field vectors** of \vec{H} and \vec{B} have only radial components. The flux density in the air gap is given using the number of turns per coil N_c and the coil current I_c :

$$B_{\delta} = \mu_0 H_{\delta} = \mu_0 \frac{\Theta}{2\delta} = \mu_0 \frac{N_c I_c}{2\delta} \quad (2.16)$$

The total **magnetic flux** across the closed surface A in the air gap around the cylindrical rotor has to be zero. As the face surfaces are neglected, it is:

$$\oint_A \vec{B} \cdot d\vec{A} = I_{Fe} \int_{x=0}^{2p\tau_p} B_{\delta}(x) dx = 0 \quad (2.17)$$

Result:

The “total area” beneath the field graph $B_{\delta}(x)$ of the air gap and the x -axis along the circumference of the machine has to be zero. Positive and negative “areas” that correspond to the positive and negative flux $\Phi' = \Phi/l$ per axial unit length, have the same magnitude $B_{\delta} \cdot \tau_p$ (Fig. 2.5).

Example 2.2-1:

Circuitual law: data for Fig 2.4: $N_c = 100$, $I_c = 10$ A, $\delta = 1$ mm, $\mu_{Fe} \rightarrow \infty$. Field lines of B are given by a closed loop C :

$$B_{\delta} = \mu_0 \frac{N_c I_c}{2\delta} = 4\pi \cdot 10^{-7} \cdot \frac{100 \cdot 10}{2 \cdot 0.001} = \underline{0.63 \text{ T}}$$

c) Magnetic Voltage $V(x)$ and Electric Loading $A(x)$:

The field graph $B_{\delta}(x)$ of the flux density in the air gap (Fig 2.4) is, after division by μ_0 , also the field graph of the magnetic field strength $H_{\delta}(x)$ and, because of the constant air gap width δ also the graph of the product $\delta H_{\delta}(x)$. As H_{Fe} is zero if $\mu_{Fe} \rightarrow \infty$, the field lines of H_{δ} arise at the rotor surface and end at the stator surface, as, in the case of an electric plate capacitor (distance of the plates δ), the field lines of the electric field E arise at the positive plate surface and end at the negative plate surface. Therefore, the following analogy is defined: “Magnetic voltage” (also called: magnetomotive force *m.m.f.*)

$$\text{“magnetic voltage” in the air gap: } \boxed{V_{\delta} = H_{\delta} \cdot \delta} \quad (2.18)$$

“electric” voltage of a capacitor: $U = E \cdot \delta$

Result:

With $\mu_{Fe} \rightarrow \infty$, the graphs of $B_{\delta}(x)$ and $V_{\delta}(x)$ are the same except for the factor μ_0/δ

$$\boxed{B_{\delta}(x) = \mu_0 \frac{V_{\delta}(x)}{\delta}} \quad (2.19)$$

The graph $V_{\delta}(x)$ “jumps” by the value of Θ at the location x where the **ampere-turns of the slot** Θ are located (Fig. 2.5). Here, “ \otimes ” signifies that the current direction into the paper layer (arrow of direction “seen from the back” = Θ negative), whereas “ \bullet ” denotes the opposite direction (arrow of direction “seen from ahead” = Θ positive). Fig. 2.6 shows exemplary a section of the slots along the air gap and the corresponding magnetic voltage $V_{\delta}(x)$ and air gap flux density $B_{\delta}(x)$, for an arbitrarily chosen arrangement of slot ampere-turns.

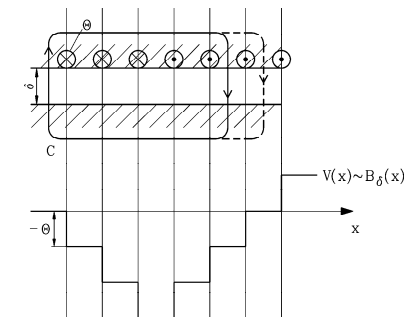


Fig. 2.6: Determination of the graph $B_{\delta}(x)$ at a given distribution of the slot ampere-turns (stator, rotor and air gap of the machine shown in plane view)

The slot ampere-turns are considered concentrated in a single point per slot respectively. Therefore, the result is a graph in the form of steps (“**field steps**”). The current density in an individual coil in the slot is infinitely large. The slot itself is infinitely small. The width of the slot b is zero, and the influence of the slot openings on the form of the graph is negligible. This idealisation means: Along x , each slot current is a *DIRAC* impulse with infinitely high “ampere-turns per unit length”:

$$A = \lim_{b \rightarrow 0} \frac{\Theta}{b} \quad \text{inside a slot,} \quad A = 0 \quad \text{outside a slot} \quad (2.20)$$

A is called “**electric loading**” (unit: “ampère/meter”). It is a function of the circumferential coordinate x . In Fig. 2.6, the electric loading $A(x)$ is an equally spaced series of *DIRAC*-“impulses” with positive and negative signs. Using (2.20), it can be derived that the integral of A yields the distributed ampere-turns. Therefore, the field graph B_δ can be calculated from $A(x)$:

$$B_\delta(x) = \mu_0 H_\delta(x) = \frac{\mu_0}{\delta} \int_0^x A(x) dx = \frac{\mu_0}{\delta} (V(x) - V_0) \quad (2.21a)$$

$$V(x) = \int_0^x A(x) dx + V_0 \quad \text{respectively} \quad A(x) = dV(x)/dx \quad (2.21b)$$

The constant V_0 has to be chosen to meet equation (2.17), hence that the positive and negative areas between the graph of $V(x)$ and the x -axis are the same, e.g., it is $V_0 = 0$ in Fig. 2.5.

d) *Magnetic Field of Coil Groups:*

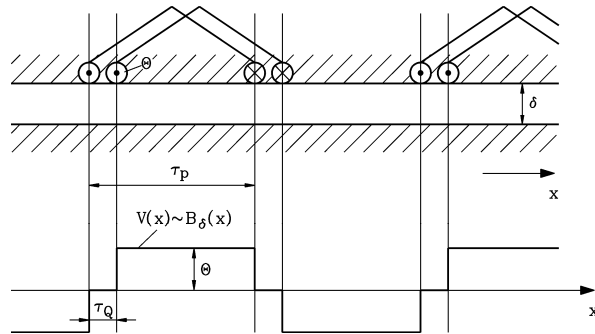


Fig. 2.7: Magnetic voltage $V(x)$ and air gap flux density $B_\delta(x)$ of a series of coil groups

Generally, the turns of a winding per pole are not concentrated in a single slot, but are distributed over a series of coils that are connected in series (**series connected coil group**). In the case of more than two poles, the coil groups can be connected in series. Each coil group of Fig. 2.7 consists of two coils with the same width (**coil width $W = \text{pole pitch } \tau_p$**) that are arranged at the distance of one **slot pitch τ_q** . The individual coil groups are allocated at the distance of one pole pitch along the circumference of the machine and connected in series. Therefore, the “concentrated” ampere-turns per coil have always the same absolute value Θ .

The corresponding graph with the form of steps is determined according to (2.21a). The horizontal axis is determined so that the positive and negative areas given by the graph have the same absolute values to meet (2.17). The integration constant V_0 is zero. The graph is **symmetrical to the abscissa**, as shown in Fig. 2.5. That is, the graphs above and below the abscissa (x -axis) are identical, if the part of the graph above the abscissa is shifted by τ_p to the left or right.

$$B_\delta(x \pm \tau_p) = -B_\delta(x) \quad (2.22)$$

In a physical way, this means that the **north and the south pole have the same shape**. In most cases, electric machines are built in this way.

2.3 Generation of Rotating Magnetic Fields

a) *Magnetic Alternating Field:*

If the coil arrangement of Fig. 2.7 is not supplied with a dc-current I_c , but with an alternating current i_c , changing sinusoidally with time (amplitude \hat{I}_c , frequency f , angular frequency $\omega = 2\pi f$)

$$i_c(t) = \hat{I}_c \cos \omega t \quad , \quad (2.23a)$$

then, the air gap field also changes sinusoidally with time according to (2.16). The field **maintains its spatial distribution** (the distribution along x), but the value of the radial field component at the coordinate x changes between its maximum positive and negative values.

$$B_\delta(x, t) = B_\delta(x) \cos \omega t \quad . \quad (2.23b)$$

The **steady-state, time-invariant** magnetic field has thus become a stationary, time-varying (with frequency f) **alternating field**.

b) *Magnetic Rotating Field:*

A rotating field may be “constructed” from the alternating field of (2.23b), by means of other – spatially distributed – coils, which are fed with alternating currents with different phase angles. In Fig. 2.7, two coil sides of two additional winding branches may be added between the two coil sides of the shown winding branch. These are also evenly distributed and full-pitched (coil pitch = pole pitch). The first winding branch is called “phase U”, the other two are named “phase V” and “phase W”. The spatial positive current direction per winding branch is chosen in the way that the displacement between phases V and U is $2\tau_p/3$, and between phase W and V twice as much, which is $4\tau_p/3$ (Fig 2.8, above). Both coil sides per coil group of phase U with positive current direction are called “**phase band**” +U, those with negative current direction “phase band” –U. The phases V and W are named in an analogous way. Thereby, **six phase bands**, successively +U, –W, +V, –U, +W, –V, are given per pole pair, where a pole pair equals a segment of $2\tau_p$ of the circumference of the machine in the air gap. This series repeats identically along the circumference as many times as the machine has pole pairs. In this example each phase band contains two coils, one per slot. The described arrangement has two slots per pole and phase (“**number of slots per pole and phase**” $q = 2$).

If the spatially distributed (distance $2\tau_p/3$ between two phases) windings of the phases U, V, W are supplied with alternating currents with different phase angles $i_U(t)$, $i_V(t)$, $i_W(t)$, where the phase shift is $T/3$ ($T = 1/f$: period time of the alternating current), a **rotating field** is generated.

$$i_U(t) = \hat{I} \cos(\omega t + \varphi) \quad (2.24)$$

$$i_V(t) = \hat{I} \cos(\omega t + \frac{\omega T}{3} + \varphi) \quad (2.25)$$

$$i_W(t) = \hat{I} \cos(\omega t + \frac{2\omega T}{3} + \varphi) \quad (2.26)$$

$$i(t) = \text{Re}\{\underline{I} \cdot \sqrt{2} \cdot e^{j\omega t}\} = \text{Re}\{I \cdot e^{j\varphi} \cdot \sqrt{2} \cdot e^{j\omega t}\} = \hat{I} \cos(\omega t + \varphi) \quad (2.27a)$$

$$\underline{I} = I \cdot e^{j\varphi} \quad (2.27b)$$

Fig. 2.8 shows the generation of a rotating field graphically. The currents $i(t)$ flowing at a given moment t in the winding branches can be calculated using **complex numbers**, where the alternating currents given by (2.24) – (2.26) are seen as phasors \underline{I} of the complex plane that rotate with the angular velocity ω (2.27). The instantaneous values $i(t)$ are given by the projection of the phasors onto the real axis (vertical axis in Fig. 2.8).

The phase angle φ (which can be chosen arbitrarily) is set to zero. Then, the current of phase U of Fig 2.8 has it's maximum positive value at the time $t = 0$, and the currents of phases V and W are only half as large and have negative signs. The corresponding slot ampere-turns and the graphs of the magnetic flux density $B_\delta(x)$ and the magnetic voltage $V_\delta(x)$ are shown on the left. Somewhat later – at the time $t = T/12$ – the currents of the phases U and V have the same absolute value but opposite signs, and the current of phase W is zero. The corresponding graph has changed its form. However – and this is very important – the north and south poles have travelled **to the left** (distance $2\tau_p/12$). At the time $T/6$, the original form of the graph is obtained again, now shifted by $2\tau_p/6$ to the left. This shows that the field is travelling two pole pitches during one period. With a linear arrangement of stator and rotor, the field travels with the velocity v_{syn} (**synchronous wave velocity**).

$$v_{syn} = \frac{2\tau_p}{T} = 2f\tau_p \quad (2.28)$$

This is given in case of **linear motors** with a linearly moving part (e. g. drive of the magnetic levitation train *TRANSRAPID*).

Example 2.3-1:

Magnetic levitation train *TRANSRAPID*: $\tau_p = 258$ mm, $f = 270$ Hz (output frequency of the inverter): $v_{syn} = 2f\tau_p = 2 \cdot 270 \cdot 0.258 = 139.3$ m/s = 501.6 km/h cruising speed

In case of a rotating electric machine as it is shown “unrolled” in Fig. 2.8, v_{syn} is the circumferential velocity of the magnetic field in the stator bore. This circumferential velocity corresponds to the synchronous angular velocity Ω_{syn} , respectively the **synchronous speed** n_{syn} of the rotating field.

$$\Omega_{syn} = 2\pi n_{syn} = \frac{v_{syn}}{d_{si}/2} = \frac{v_{syn}}{p\tau_p/\pi} = \frac{2\pi f}{p} = \frac{\omega}{p} \quad (2.29)$$

$$n_{syn} = \frac{f}{p} \quad (2.30)$$

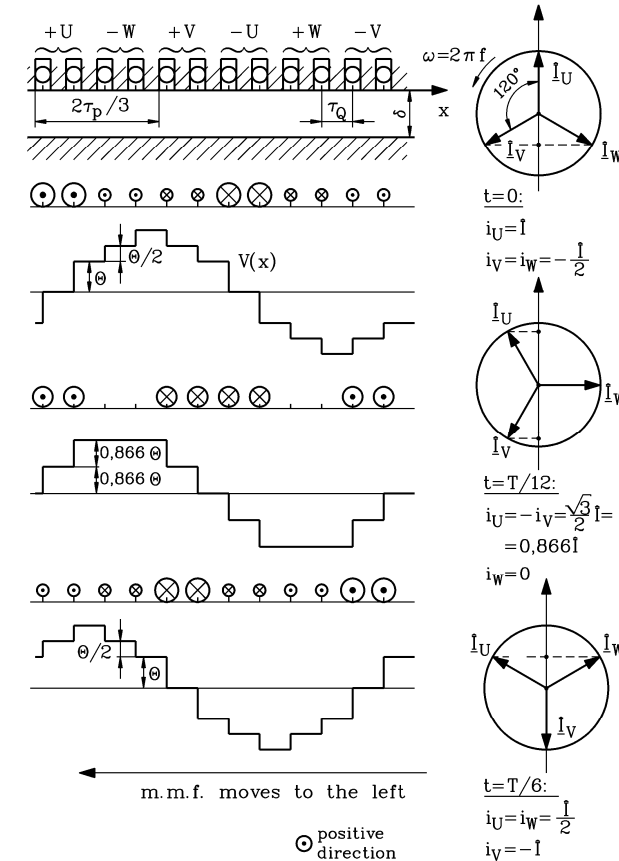


Fig. 2.8: A winding system of three winding branches, displaced by $2\tau_p/3$, and fed with alternating currents with $T/3$ phase displacements, generates a travelling magnetic field (linear motor) or a rotating magnetic field (machine with rotating fields, polyphase machine).

Example 2.3-2:

Supply of the winding branches with alternating currents with frequency $f = 50$ Hz:

- Two-pole machine ($2p = 2$): rotating field rotates with $n_{syn} = 50$ Hz = 3000/min
- Four-pole machine ($2p = 4$): $n_{syn} = 25$ Hz = 1500/min
- Sixty-pole hydro-generator ($2p = 60$): $n_{syn} =$ 100/min

Example 2.3-3:

USA and Japan use grids with 60 Hz:

- Two-pole machine ($2p = 2$): rotating field with $n_{syn} = 60\text{Hz} = 3600/\text{min}$
- Four-pole machine ($2p = 4$): $n_{syn} = 30\text{ Hz} = 1800/\text{min}$
- Sixty-pole hydro-generator ($2p = 60$): $n_{syn} = 120/\text{min}$

	$2p$	-	2	4	6	8	10	12	14
$f = 50\text{ Hz}$	n_{syn}	1/min	3000	1500	1000	750	600	500	428.6
$f = 60\text{Hz}$	n_{syn}	1/min	3600	1800	1200	900	720	600	514.2

Table 2.1: Typical synchronous speed at 50 Hz and 60 Hz frequency

Remark:

The direction of travel / rotation of Fig. 2.8 changes, when the currents of two phases are interchanged. You can verify this by yourself by drawing a figure in analogy to Fig. 2.8, where the current i_W flows in phase V and the current i_V in phase W.

Result:

The direction of rotation of a rotating field can be reversed by interchange of two phases.

2.4 Winding Arrangements

a) Single-Layer Winding:

How are the coils to be arranged in the slots of the stator lamination for rotating fields to be generated? Fig. 2.8 shows a **three phase winding** (phases U, V, W, phase number $m = 3$). This winding has **six phase bands** (three phase bands +U, +V, +W, three phase bands -U, -V, -W). Initially, the number of slots per coil and phase q , hence the number of coils per phase band, can be chosen arbitrarily. The total number of slots of the stator Q of an electric AC machine is determined by the number q :

$$Q = 2pmq \tag{2.31}$$

Each slot of the winding shown in Fig. 2.9 contains only the winding of one coil. Therefore, this winding is called **single-layer winding**. Each coil group generates a north and a south pole, thus two coil groups per phase are needed to obtain four poles.

The coils may have identical geometry; then, the **coils have identical span**. As an alternative, the coils that are connected in series within a coil group can be designed as **concentric winding**. This does not change the distribution of the slot ampere-turns (Fig. 2.9). Concentric winding is very suitable for machines wound by robots, as it is generally the case with small machines.

Example 2.4-1:

Three phase, 12-pole machine with $q = 3$ coils per coil group:

- number of slots: $Q = m2p'q = 3 \cdot 12 \cdot 3 = 108$

Example 2.4-2:

Fig. 2.10: unrolled stator bore of a four-pole machine:

- $2p = 4, m = 3, q = 2$: number of slots $Q = 24$
- design with concentric coils

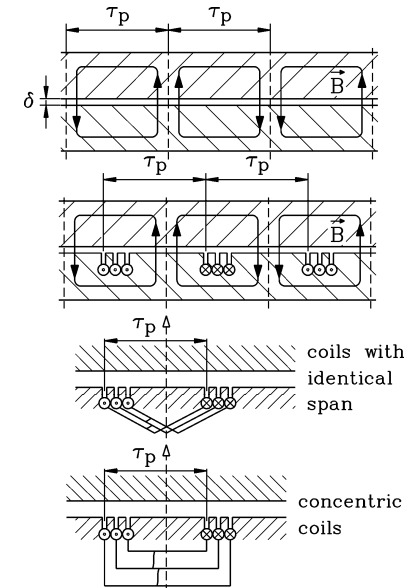


Fig. 2.9: Winding branch with $q = 3$ coils: coils with identical span $W = \tau_p$ and concentric coils

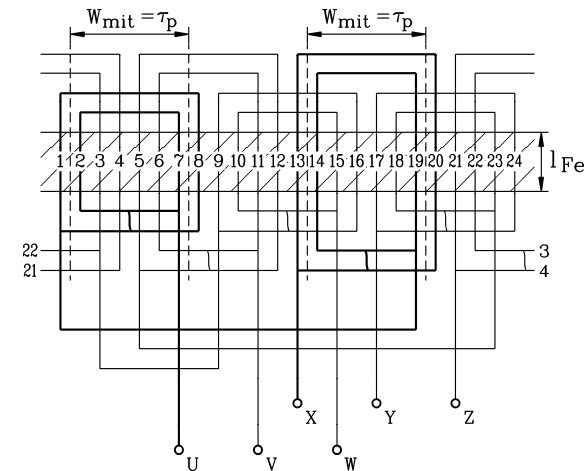


Fig. 2.10: Three-phase **single-layer winding** with **concentric** coils ($2p = 4, m = 3, Q = 24, q = 2$) designed as two-level winding with short and long coils

The view of the winding of Fig. 2.10 shows the **problem of single-layer windings**: The winding overhang, which is the part outside the lamination where the coils have to cross, does not provide room for the crossing, because all coils are at the same level. Therefore, the

winding overhangs of some coils have to be bent. One possible remedy is shown in Fig. 2.10. Here, the end connections are designed alternately with a short and a long winding overhang. The coils with the longer end connection can be bent easily. However, with this technique, at least four poles are needed for each phase to have *the same length of the winding* and therefore the same resistance.

In the lateral view of the winding overhang, the short coils are at the level of the slots and the end connections of the long coils are on a second level (“**two-level-winding**”).

Example 2.4-3:

Fig. 2.11: Poly-phase winding of the *TRANSRAPID*-linear-stator: $m = 3, q = 1$. All coils U, V, W have the same length, which is different than the winding of Fig. 2.10. The terminals of coil U are always at the level of the slot, those of coil W always bent upwards (2nd “level”), those of coil V bent in the shape of an “S”.

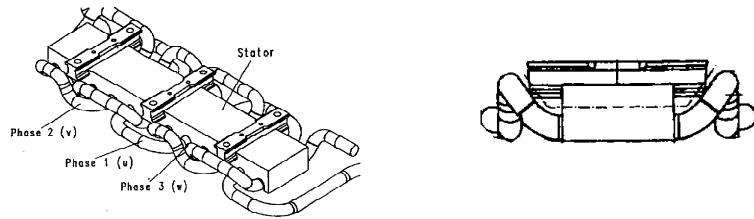


Fig. 2.11: Three phase **single-layer winding** with **wave-wound** coils ($N_c = 1$) of the *TRANSRAPID* magnetic levitation train ($m = 3, q = 1$)

Low-cost single-layer windings combined with (generally concentric) coils of **round-wire copper** are used with low-voltage machines of small and medium power.

b) Two-layer winding:

Form-wound coils with rectangular cross section are used with larger machines at rated power typically $> 0.5 \dots 1$ MW and high-voltage windings (“high voltage” is defined as rated voltage > 1 kV). These are designed as **two-layer windings** with identical span. Fig. 2.12 shows that the ampere-turns of Fig. 2.9 with $q = 3$ coils per coil group can also be realised with **two** coil sides of different coils arranged one upon the other in one slot. The ampere-turns Θ of the slot are generated by the two coil sides together.

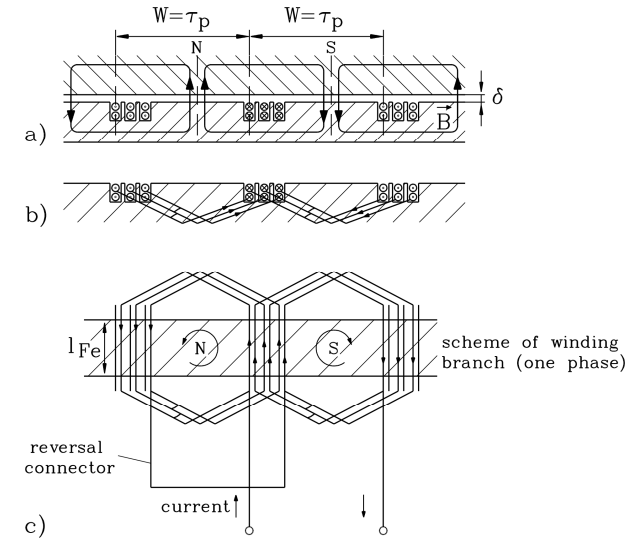


Fig. 2.12: Winding branch of a fully-pitched two-layer winding with $q = 3$

With this type of winding, north and south pole are generated by **two** coil groups. Therefore, the winding direction of the coil group of the south pole has to be opposite to the one in the north pole. This is realised by **reversal connectors** in the area of the end winding (Fig. 2.12), that connect coil groups of a north and a south pole. Thus, four coil groups are needed for four poles.

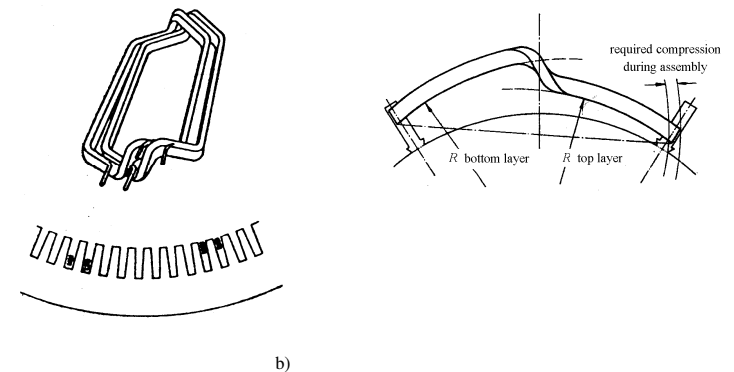


Fig. 2.13: Form-wound coils of a two-layer winding: a) two form-wound coils before insertion into the slots of the lamination: no cross-over points exist in the winding overhang, b) form-wound coil after insertion into a slot

Cross-over in the winding overhang is avoided by use of the two layer design, because the coils always change between upper and lower layer. Therefore, they have to be bent in a specific way as **form-wound coils**. Thereby, the winding overhang is a regular (“balanced”) arrangement of the end connections that change from the upper to the lower layer (Fig. 2.13).

The preformed form-wound coils have to be inserted thoroughly into the slots. These cannot be pulled into the slots by robots or by hand as it is the case with random-wound coils (Fig. 2.13b). Special attention has to be given to the insertion of the last coil, because the coil side of the lower layer has to be inserted below the coil side of the upper layer of the already inserted coil. With very large machines that often have single-turn coils ($N_c = 1$), this is only possible with the coils split into two coil sides (“bars”). First, all bars of the lower layer are inserted, next, all bars of the upper layer. Then, the bars are connected at the end winding overhang by brazing.

c) *Series and Parallel Connection of Coil Groups:*

The coil groups are connected to phases, which can be done as **series and parallel** connection of the coil groups.

Example 2.4-4:

Eight-pole machine:

Two-layer winding: 8 coil groups with q coils per phase are given.

Possible connections:

- $a = 1$: series connection of all 8 coil groups
- $a = 2$: 4 coil groups in series, parallel to the 2nd series of coil groups
- $a = 4$: 2 coil groups in series, 4 parallel series of coil groups
- $a = 8$: all 8 coil groups connected in parallel

Single-layer winding: 4 coil groups with q coils per phase are given.

Possible connections:

- $a = 1$: series connection of all 4 coil groups
- $a = 2$: 2 coil groups in series, parallel to the 2nd series of coil groups
- $a = 4$: all 4 coil groups connected in parallel

Hence, the magnetically effective **number of turns per phase** N is (with the number of turns per coil N_c):

$$N = \frac{pqN_c}{a} \quad \text{Single-layer winding} \quad (2.32)$$

$$N = \frac{2pqN_c}{a} \quad \text{Two-layer winding} \quad (2.33)$$

Example 2.4-5:

Four-pole machine, $q = 2$, 11 turns / coil ($N_c = 11$), series connection of all coil groups: $a = 1$ (Fig. 2.15):

Number of turns per phase $N = 4 \cdot 2 \cdot 11 / 1 = 88$ turns.

d) *Short-Pitching of Coils:*

The **two-layer winding** allows another degree of freedom of the design of the winding, which is the **design of short-pitched coils**. Fig. 2.14 shows that the coil width W can be shorted by the number of slots S .

$$W = \tau_p \cdot \frac{m \cdot q - S}{m \cdot q} = \tau_p \cdot \frac{Y_Q}{m \cdot q} \quad (2.34)$$

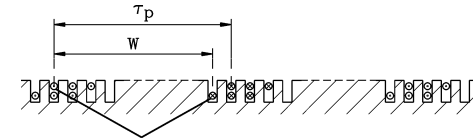


Fig. 2.14: Coil group as of Fig. 2.12 but with coil width one slot shorter than the pole pitch (“short-pitched” coil)

It will be shown in Chapter 3 that short-pitching allows to obtain field distributions that are closer to the wanted ideal sinusoidal distribution.

Example 2.4-6:

Short-pitched two-layer polyphase winding: four-pole machine, $m = 3$, $Q = 24$, $q = 2$: short-pitching is possible for $S < mq = 3 \cdot 2 = 6$: $S = 1, 2, 3, 4, 5$.

It is $S = 1$, hence $W/\tau_p = 5/6$ in Fig. 2.15.

Short-pitching of $W/\tau_p < 2/3$ is generally avoided, because of a too small flux linkage of a coil in this case.

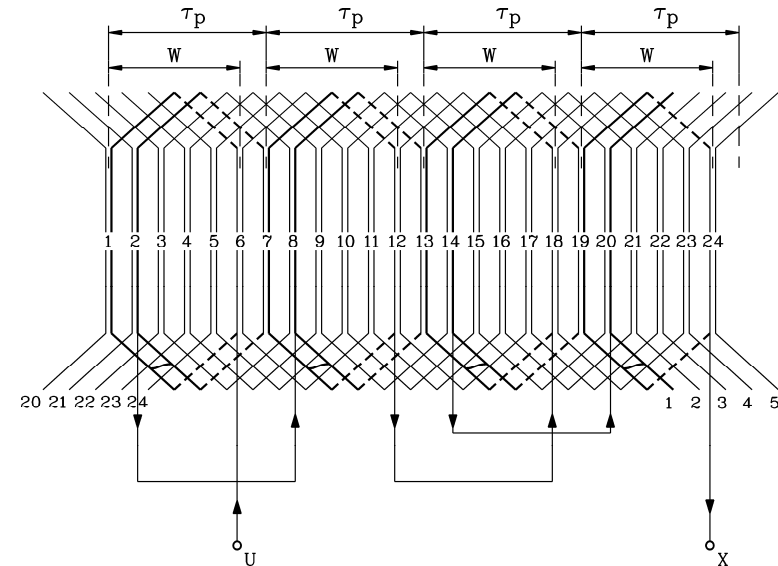


Fig. 2.15: Winding scheme of a short-pitched two-layer winding for $2p = 4$, $m = 3$, $Q = 24$, $q = 2$, $W/\tau_p = 5/6$

e) *Wye (Y, Star) and Delta Connection:*

First, the end windings of the three phases (Fig. 2.15) U-X, V-Y, W-Z are not connected: Depending on the demand, they can be connected as delta or as star connection.

Wye (star) connection:

Star point X-Y-Z shorted, U, V, W connected to the grid

Delta connection:

X-V, Y-W, Z-U connected respectively and connected to the grid.

f) *Phase Numbers others than $m = 3$:*

In Fig. 2.8, the **rotating field** is generated by a system of $m = 3$ alternating currents with $T/3$ phase displacement ($\omega T/3 = 120^\circ$) flowing in winding branches with $2\tau_p/3$ spatial displacement. Generally, such a rotating field can also be generated by a system of m alternating currents with T/m phase displacement flowing in m winding branches with $2\tau_p/m$ spatial displacement. In the area of electrical power engineering, the number of phases $m = 3$ has become well-established, because of economical reasons. However, machines with rotating fields designed with a single phase ($m = 1$), two ($m = 2$) and several phases ($m > 3$, e.g. $m = 6$) also exist.

Single-phase synchronous generators used for railway applications in the single-phase grid of the railways (15 kV, 16,7 Hz) are designed as **single-phase** machines, as well as small synchronous motors for clocks (micro motors).

Induction motors for the single-phase grid (230 V, 50 Hz) are designed as **two-phase** machines. Here, the second phase is connected to the grid via a capacitor C to get the necessary phase shift of 90° for the phase current of the second phase. The first phase is connected directly to the grid ("**Single-phase induction motor**", **capacitor motor**), Fig. 2.16.

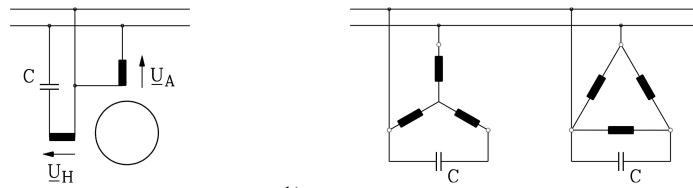


Fig. 2.16: Motor operation at a single-phase grid:

- "**Single-phase motor**" (two phase winding) with "working" (A) and "auxiliary" (H) phase and capacitor C ,
- "**STEINMETZ**" connection: A three-phase motor (star or delta connection) supplied from a single-phase grid only generates a rotating field with use of a capacitor C that shifts the phase of the three phases artificially. As the phase shift differs significantly from 120° , the rotating field rotates non-uniformly and the field amplitude oscillates heavily (only useful for small motors).

Large induction and synchronous motors in the range of some MW rated power are often designed with **six phases**. The feeding six phase system is generated via a transformer and/or a converter from the three-phase system.

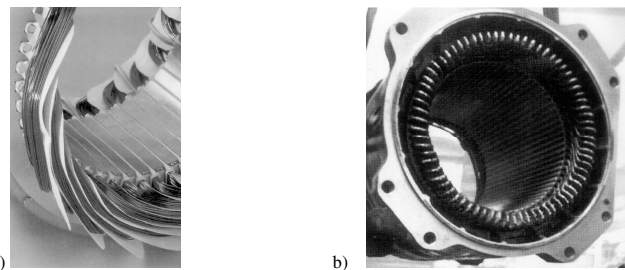


Fig. 2.17: Winding overhang of poly-phase windings which are embedded in the stator lamination: a) round-wire two-layer winding of a small industrial induction motor, b) form-wound two-layer winding of a 1.6 MW induction motor designed as a locomotive - drive